

# Study of the Thermodynamic Functions of the Adsorption of Safranin Dye from Water Using Cellulose after Loading it with Silver Nanoparticles Prepared by the Green Method

Atheer Ali Salem Hussein, Liqaa Hussain Alwan

Samarra University, College of Education, Department of Chemistry

**Received:** 2025, 15, Apr

**Accepted:** 2025, 21, May

**Published:** 2025, 23, Jun

Copyright © 2025 by author(s) and BioScience Academic Publishing. This work is licensed under the Creative Commons Attribution International License (CC BY 4.0).



Open Access

<http://creativecommons.org/licenses/by/4.0/>

**Annotation:** Silver nanoparticles were prepared using a plant extract obtained from the leaves of the La Niña tree, where the extract was used as a natural reducing agent due to its content of flavonoids and antioxidants. The nanoparticles were synthesized through the reaction of silver nitrate with the plant extract under controlled thermal conditions with continuous stirring. These particles were characterized using FT-IR, EDX, SEM, and XRD techniques, which confirmed the formation of silver nanoparticles with Ag–O bonds and an average size of approximately 18.5 nanometers. Spectral analyses showed the presence of organic functional groups remaining from the plant extract.

Additionally, the adsorption of Safranin dye on the surface of cellulose loaded with the nanoparticles was studied. The maximum wavelength of the dye was determined at 518 nanometers, and calibration curves were prepared to determine dye concentrations. The study showed that the adsorption equilibrium time was reached within 20–25 minutes, with a high adsorption efficiency (about 92% without nanoparticles, and 85.5% with their presence). Thermal analyses indicated that the adsorption process was exothermic and spontaneous, with negative entropy changes reflecting an increase

in order during adsorption.

These results suggest the effectiveness of using the plant extract in preparing environmentally friendly silver nanoparticles and their ability to enhance the adsorption properties of cellulose for dye removal from aqueous solutions.

**Keywords:** water pollution, cellulose, adsorption.

## Introduction

Water pollution is considered one of the most serious problems facing humanity due to the diversity of its sources and the rapidity of its spread [1]. Among the major contributors to water contamination are dyes, owing to their extensive use in the textile industry, photographic pigments, and various highly colored organic compounds. Dyes are also widely used in the food, pharmaceutical, and other industries, where they are produced in multiple forms [2]. Nanotechnology is an emerging field with wide-ranging applications in the treatment of environmental pollutants. Advances in nanoscale science offer unprecedented opportunities for developing more cost-effective and environmentally acceptable water purification processes. In recent years, considerable attention has been directed toward the synthesis and application of nanostructured materials as adsorbents for removing toxic and harmful compounds from water and wastewater, through the adsorption of pollutants using nanomaterials [3]. Additionally, nanomaterials can be employed as antibacterial agents during water treatment processes [4].

**Cellulose** is the most abundant and environmentally sustainable biopolymer, and it is a principal component of the woody plant cell wall. Chemically, cellulose is a carbohydrate composed of a linear chain of D-glucose units [5]. It is the most widespread organic compound in nature and is characterized by remarkable chemical stability. Cellulose is an insoluble, tasteless, odorless, and hydrophilic polymer. It exhibits a highly crystalline structure and is notoriously difficult to dissolve in organic solvents, as illustrated in Figure (1).

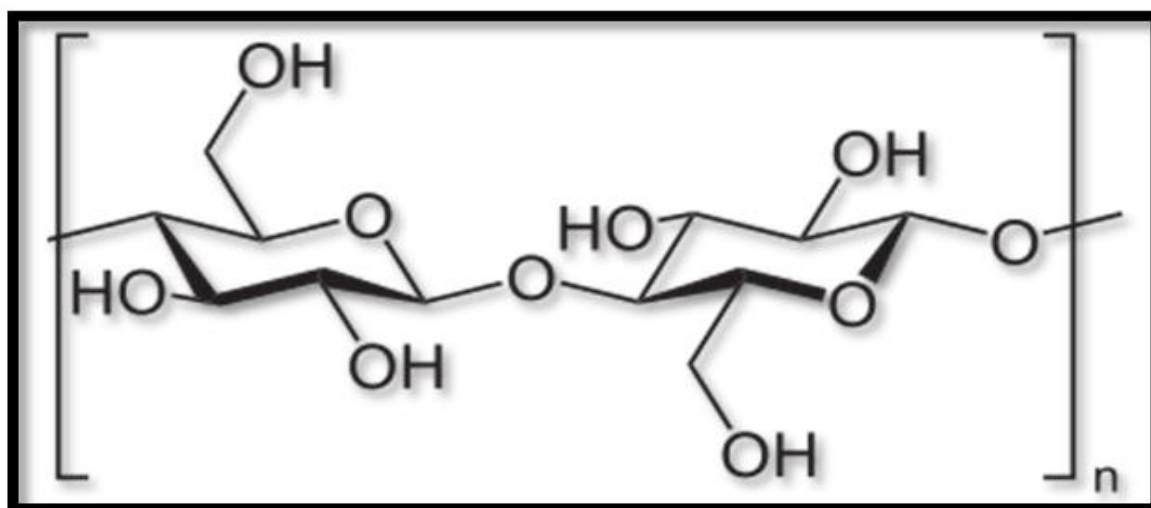


**Figure (1) The chemical formula of cellulose**

**Silver Nanoparticles** have gained significant attention due to their wide range of applications, such as surface disinfection, drug delivery, dental materials, wound healing, cosmetics, water purification, and more. This is due to their low toxicity to human health while being highly toxic

to microorganisms. Figure (2) illustrates some of the applications of silver nanoparticles [6].

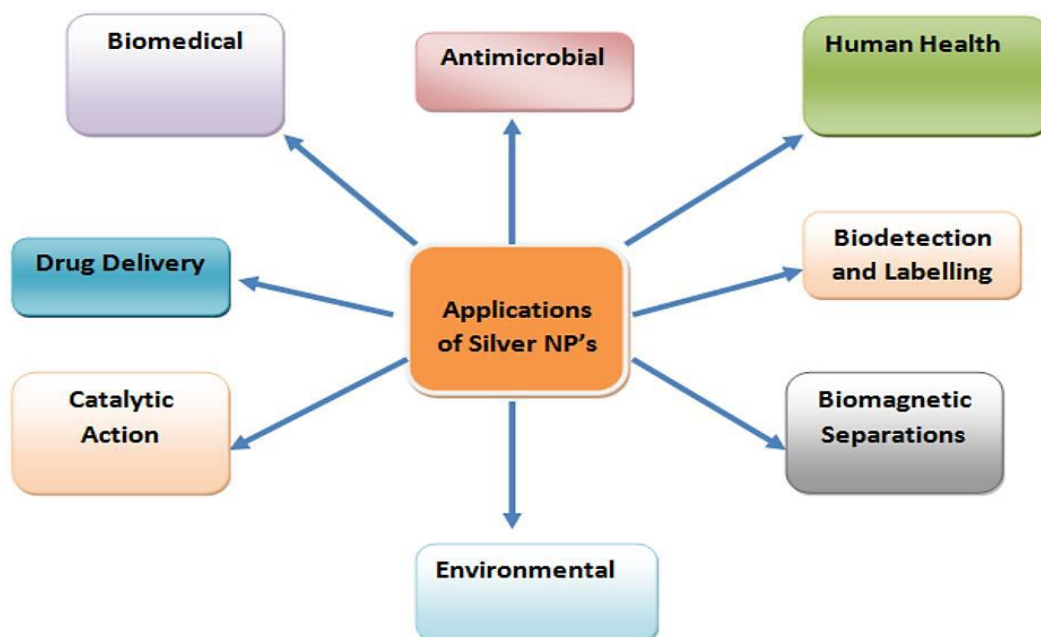


**Figure (2): Some applications of silver nanoparticles**

Currently, silver nanoparticles are relied upon for their effective impact on these organisms. Their physical and chemical properties, such as size and shape, play a crucial role in disrupting or killing microorganisms. Therefore, silver nanoparticles have wide applications and exhibit strong antimicrobial effects. In environmental remediation, air filters based on silver nanoparticles have been developed, reducing the problem of biological pollution caused by airborne bacteria and fungi [7][6]. **Safranin Dye** is a pigment that can bind well to the materials they are intended to color, imparting pure color to them. It has been found that a large amount of these dyes is released as wastewater or soil. The environmental behavior of these dyes is very dangerous because of the raw materials from which they are made, such as aniline, benzene, toluene, and amino compounds, as they are carcinogenic substances and can be regenerated as a result of the decomposition of dyes or due to some biological reactions [8]. Safranin dye is a dye with a molecular weight of 350.84 g/mol and its chemical formula is  $C_{20}H_{19}ClN_4$ . It is one of the basic dyes that combine with acidic radicals such as acetate radicals and chlorides...etc., and it contains amino alkyl groups as shown in its formula in Figure (3). It is very important for plant tissues, as it can stain all plant tissues, such as lignin, suberin, xylem vessels, chromosomes, and nuclei, and is called nuclear dyes accordingly. It also stains animal tissues, as it stains fibers, unicellular animals, and sperm cells. Therefore, it tends to stain natural fibers (cotton and linen) and synthetic ones [9].

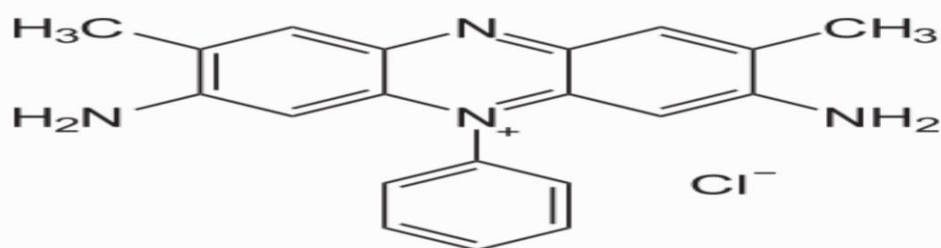


**Figure (3) Safranin dye formula**

**Adsorption** is defined as the phenomenon of the accumulation of (molecules, atoms or ions) of a liquid or gaseous substance on the surface of another solid substance, or it is the association of

material molecules in the active sites of the surface physically through van der Waals forces or chemically through the formation of chemical bonds or bonds with active sites on the surface [10]. Adsorption is also defined as the process of transferring dissolved pollutants of adsorbed materials from aqueous solutions to the surface of an adsorbent solid substance, where the degree of adsorption depends on the relationship between the surface area of the adsorbent material and the nature and size of the adsorbent material [11]. The factors affecting adsorption are the nature of the adsorbent surface, temperature, acidity function, the nature of the adsorbent material, ionic strength, and the effect of the solvent. The adsorption process is considered a surface phenomenon, unlike absorption, which is the process of penetration and diffusion of the first substance into the second substance, as in Figure (4). The two phenomena are called diffusion, which means the transfer of the substance's molecules from one phase and their accumulation in another phase. There is also another phenomenon called extortion, which includes the separation of molecules from the surface, and it is the opposite process of adsorption [12].

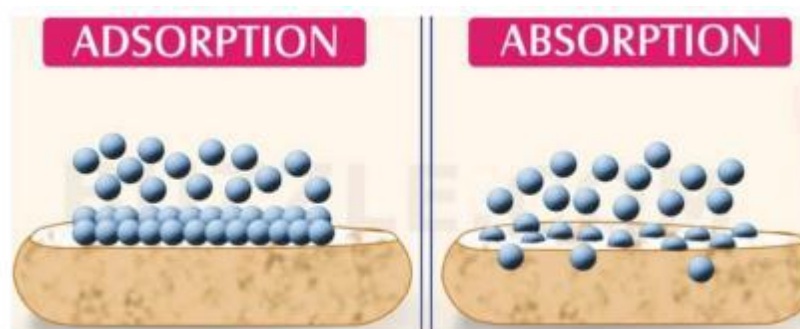


**Figure (4) The difference between adsorption and absorption**

The adsorption process is usually accompanied by a decrease in the free energy ( $\Delta G$ ) of the adsorbent surface, as well as a decrease in entropy ( $\Delta S$ ), i.e. a decrease in the randomness of the system due to the restriction of the atoms resulting from the adsorption process due to the association of the atoms or molecules of the adsorbed material with the adsorbent surface, and thus their movement decreases and their freedom is restricted from what it was before the adsorption process. Therefore, when a decrease in the standard free energy ( $\Delta G$ ) and entropy ( $\Delta S$ ) occurs at the same time, the heat content ( $\Delta H$ ) will also decrease according to the thermodynamic relationship that connects them and at the same temperature.[13]

$$\Delta G = \Delta H - T\Delta S$$

## Materials and Methods

### Equipment Used

UV-Vis spectrophotometer, pH meter, drying oven, scanning electron microscope (SEM), X-ray diffraction (XRD), energy dispersive X-ray spectrometer (EDX), temperature-controlled shaking water bath, magnetic stirrer heater, four-decimal sensitive balance, ultrasonic water bath, electronic clock, incineration furnace, filter paper, mercury thermometer.

### Materials Used

The chemicals used to prepare nanomaterials from La Niña leaves are characterized by high purity. The materials used are cellulose polymer, hydrochloric acid, sodium hydroxide, deionized water, silver nitrate, and safranin dye.

### Preparation of the Plant Extract.

The plant extract was prepared from the leaves of the La Niña tree found in the college garden by collecting samples of the leaves and washing them with plain water to get rid of the dust and dirt stuck to them. Then, they were washed with distilled water several times and then with deionized water. After completing the washing process, (7g) of leaves were mixed with 80ml of deionized water, taking into account continuous stirring using a magnetic stirrer. The mixture was heated to (80) degrees Celsius for 30 minutes, then it was filtered and the brown La Niña leaf extract was obtained as in Figure (5). The role of the plant extract is as a reducing agent through its containing a large amount of polyphenols that consist of flavonoids, antibiotics, antioxidants and organic groups. When this extract is added to the nitrate salt, it breaks the (-OH) bond and forms a partial bond with the metal. When this partial bond is broken, the electrons are transferred to form hydroxide, which quickly reacts with (-OH) coming from the nitrate to form Nano oxide.



Figure (5) Preparation of plant extract

### Preparation of silver nanoparticles.

6g of silver nitrate was dissolved in 1600ml of deionized water and the mixture was heated to 100°C for 30 minutes. The plant extract was then added dropwise to the silver nitrate solution using a burette while stirring continuously and maintaining the temperature at 100°C. After the addition process was completed, the solution was removed from the heat and left to stir for 15 minutes to form a precipitate. After 24 hours, the clear solution was discarded, retaining a small amount of it with the precipitate. It was then placed in an ultrasonic device for an hour and a half to break down the particles from the precipitate. The precipitate was placed in a drying oven for four hours at 80°C to obtain dry silver nanoparticles, as shown in the following equation.



### Determination of the calibration curve and $\lambda_{\text{max}}$ value for safranin dye.

The maximum wavelength ( $\lambda_{\text{max}}$ ), which is obtained at the highest absorbance of the safranin dye solution, was determined using a UV-Vis spectrophotometer. To obtain the calibration curve, eight aqueous solutions were prepared in 10 ml volumetric bottles at different concentrations (1, 1.5, 2, 2.5, 3, 3.5, 4, 4.5)  $\times 10^{-5}$  M. Quartz cells were used to measure the

absorbance values of all diluted safranin dye solutions after the device was zeroed on the solvent (water) as a reference (Blank) at the dye's maximum wavelength, which was plotted based on the Beer-Lambert law.[14]

Calculating the thermodynamic functions of adsorption.

The values of the equilibrium constant for the adsorption process ( $K_{eq}$ ) were calculated, representing the ratio of the concentrations of the adsorbed substance to the concentrations of the residual substance in the solution at different temperatures. From plotting the relationship  $\ln K_{eq}$  versus the reciprocal of temperature  $1/T$ , the value of  $\Delta H$  was calculated based on the (van't Hoff) equation No. (6). We obtained  $\Delta H$ , where a straight line with a slope equal to  $(-\Delta H/R)$  was obtained. From this, we obtained the values of  $\Delta S^0$  and  $\Delta G^0$  according to equations (7) and (8), respectively, as follows [15]:

1- Calculating the value of ( $\Delta H^0$ ) from plotting  $\log K$  versus the reciprocal of temperature, based on the van't Hoff equation [22] No. (6).

$$\log K = (-\Delta H^0/2.303RT) + C \text{ ----- (6)}$$

Where:

$\log K$  = logarithm of the maximum amount adsorbed (mg/g).

$C$  = van't Hoff constant

$T$  = temperature (Kelvin)

$R$  = universal gas constant (8.314) J.mol<sup>-1</sup>.K<sup>-1</sup>.

2- The value of ( $\Delta G^0$ ) was calculated from Equation No. (7).

$$\Delta G^0 = -RT \ln (Q_e/C_e) \text{ ----- (7)}$$

Where:

$R$  = universal gas constant (8.314) J.mol<sup>-1</sup>.K<sup>-1</sup>

$T$  = absolute temperature

$C_e$  = equilibrium concentration (mg/L).

$Q_e$  = amount of adsorbed substance (mg/g).

3- The value of ( $\Delta S^0$ ) was calculated from Equation No. (8).

$$\Delta G^0 = \Delta H - T\Delta S^0 \text{ ----- (8)}$$

## Results and Discussion

Characterization of the Synthesized Nanomaterials Using XRD, EDX, FT-IR, and SEM Techniques

### Characterization of Silver Nanoparticles Using FT-IR Spectroscopy:

Figure (6) presents the infrared spectrum of the synthesized silver nanoparticles, revealing several absorption bands corresponding to various functional groups. An absorption band at 468.22 cm<sup>-1</sup> is observed and attributed to the Ag–O bond, indicating the formation of silver oxide nanoparticles. Another band at 618.90 cm<sup>-1</sup> further confirms the presence of the Ag–O linkage. Additional bands at 1113 cm<sup>-1</sup> and 1269.98 cm<sup>-1</sup> may correspond to C–O or C–N groups, suggesting the presence of organic impurities, possibly from residual plant extract or the reaction medium. The band at 1382.72 cm<sup>-1</sup> is associated with CH<sub>3</sub> or NO<sub>3</sub> groups, while the band at 1464.83 cm<sup>-1</sup> corresponds to CH<sub>2</sub> vibrations. The appearance of a band at 1631.66 cm<sup>-1</sup> indicates the presence of H–O–H bending vibrations, reflecting water content in the sample. A strong absorption band at 1741.31 cm<sup>-1</sup> is attributed to C=O carbonyl stretching. Furthermore, absorption bands at 2854.45 cm<sup>-1</sup> and 2925.05 cm<sup>-1</sup> are associated with C–H stretching

vibrations, and the broad peak at  $3430.11\text{ cm}^{-1}$  suggests the presence of OH groups or hydrogen-bonded water. These findings confirm that the synthesized silver nanoparticles are chemically bound to oxygen through Ag–O linkages, indicating successful nanoparticle formation. The presence of additional bands suggests minor organic or moisture impurities, likely originating from the plant extract used in the synthesis or from ambient conditions during drying and storage.

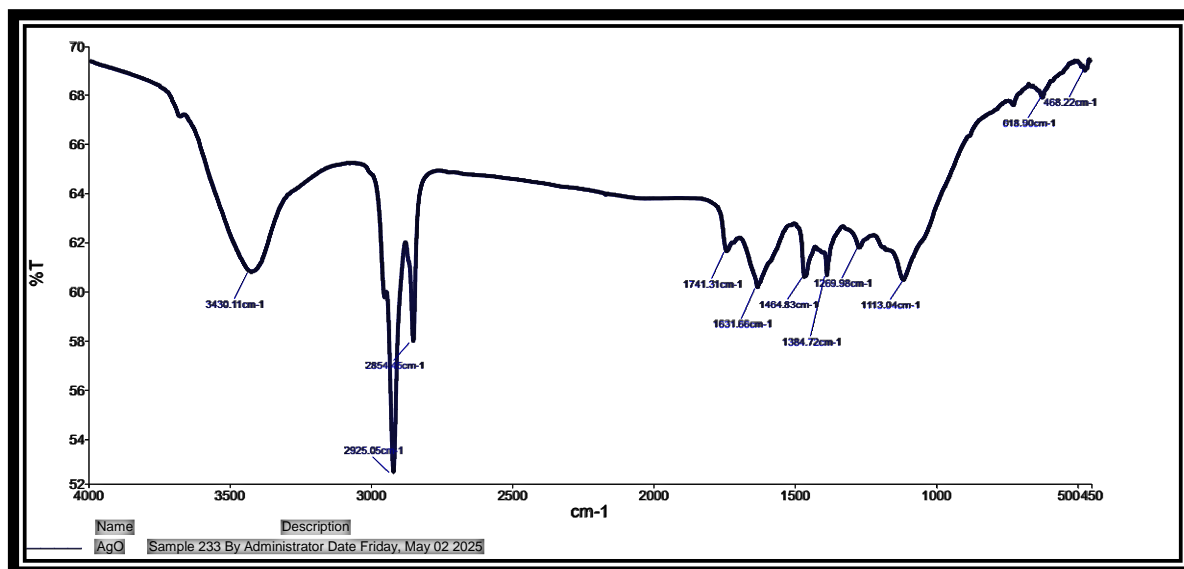


**Figure (6): Infrared spectrum of prepared silver nanoparticles**

### Energy Dispersive X-ray Spectroscopy (EDX) of Silver Nanoparticles

Energy Dispersive X-ray Spectroscopy (EDS or EDX) is a highly effective analytical technique used to determine the elemental composition and chemical characteristics of samples, as well as to assess the purity of the synthesized compounds. Figure (7) and Table (1) present the EDX analysis of the synthesized silver nanoparticles. As observed in the spectrum, a prominent peak corresponding to silver is detected, confirming the presence of silver nanoparticles with a weight percentage of 85.5% in the sample. The second peak corresponds to oxygen, accounting for 14.5% of the sample's weight. The presence of oxygen is attributed to the synthesis process, during which the *Nenia* leaf extract was exposed to an alkaline NaOH solution.

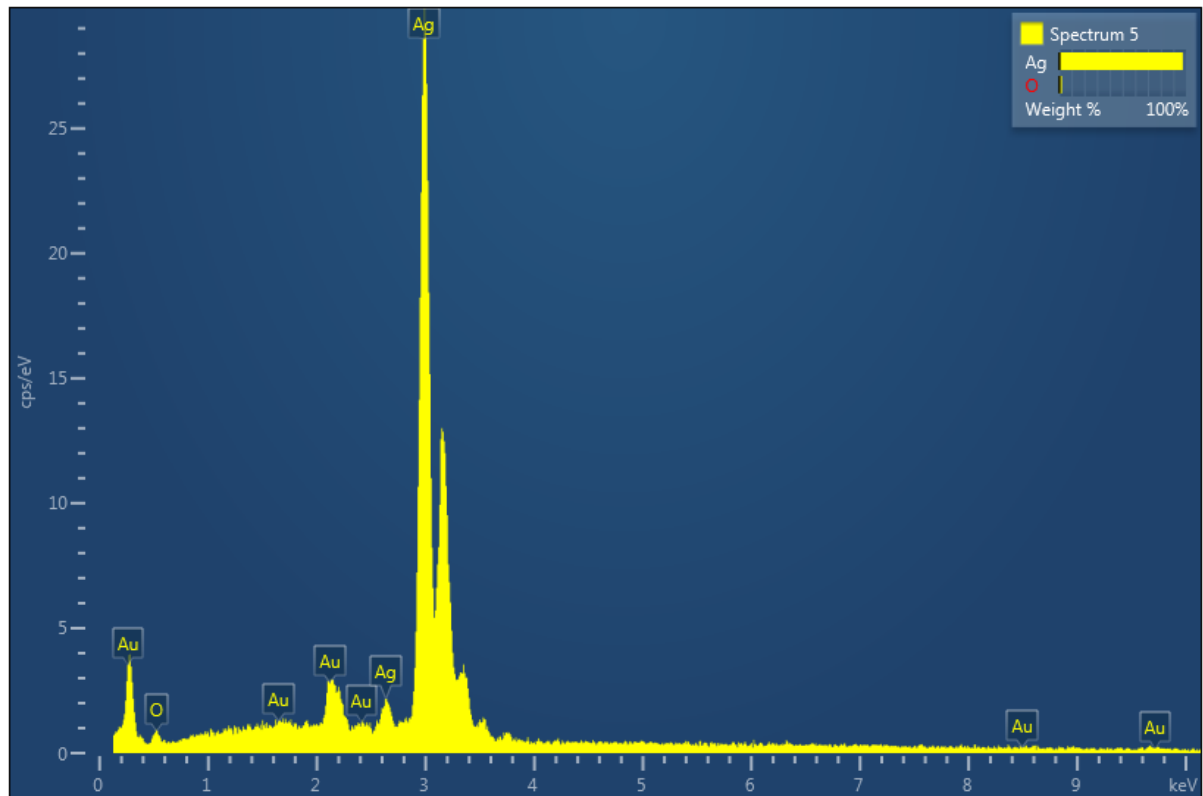


**Figure (7): Energy dispersive X-ray spectroscopy (EDX) of the prepared silver nanoparticles.**

**Table (1): Elemental percentages of the silver nanoparticles in EDX analysis.**

Element	Atomic %	Weight %
Ag	85.50	97.55
O	14.50	2.45

### Scanning Electron Microscopy (SEM) Examination of Silver Nanoparticles.

Scanning electron microscopy (SEM) is an advanced technique that relies on the use of an electron beam to study the surface morphology of a sample and determine the structures of the prepared particles. Figure (8), which shows an SEM examination of silver nanoparticles prepared from La Niña leaves in the presence of sodium hydroxide, shows clear accumulations of silver nanoparticles, which are clusters of nanoparticles of approximately uniform shape. Using SEM techniques, we can obtain information about the composition, chemical properties, and morphology of nanoparticles and other materials. These techniques are important tools for the diagnosis and analysis of nanomaterials with high accuracy and great detail.

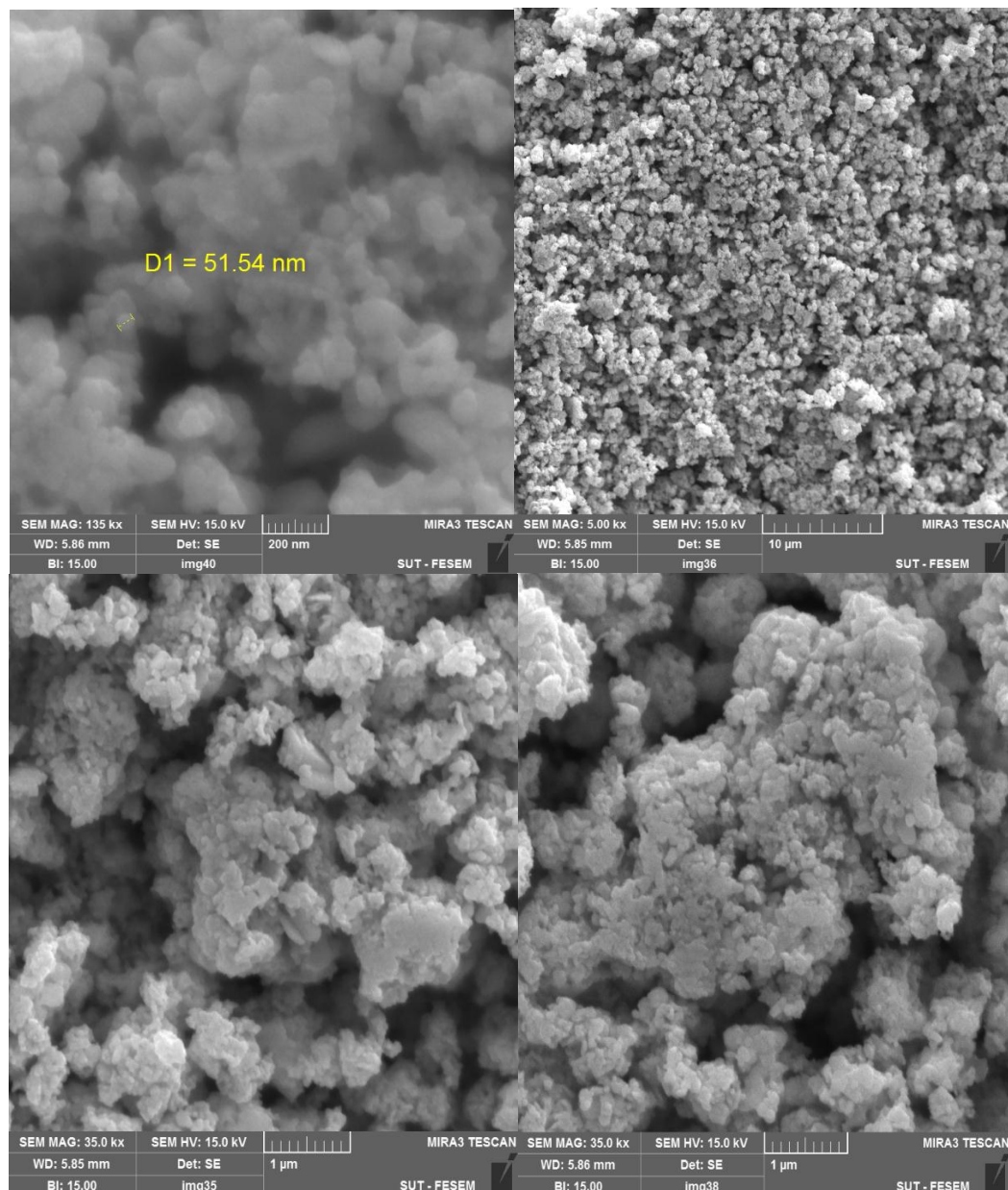


**Figure (8): Scanning electron microscope (SEM) examination of the prepared silver nanoparticles.**

### X-ray Diffraction (XRD) Measurement of Silver Nanoparticles

The synthesized silver nanoparticles from Nenia leaves were characterized using X-ray Diffraction (XRD) to determine the crystalline structure of the prepared nanoparticles and to calculate their size using the Debye-Scherrer equation [16]:

$$D = K \lambda / \beta \cos \theta$$

Where:

D is the particle size in nanometers (nm),

K is the Scherrer constant, typically taken as 0.9,

$\lambda$  is the wavelength of the X-rays used (0.15406 nm),

$\beta$  is the full width at half maximum (FWHM) of the peak in degrees, converted to radians by multiplying by  $\pi/180$

$\theta$  is the Bragg diffraction angle in degrees.

Figure (8) illustrates the XRD spectrum of the synthesized silver nanoparticles, and Table (2) presents the data obtained from the XRD analysis for the three most intense diffraction peaks. These values were used to calculate the average crystalline size of the silver nanoparticles, which was found to be 18.5 nm. Since this value is below 100 nm, it confirms that the synthesized material lies within the nanoscale range.

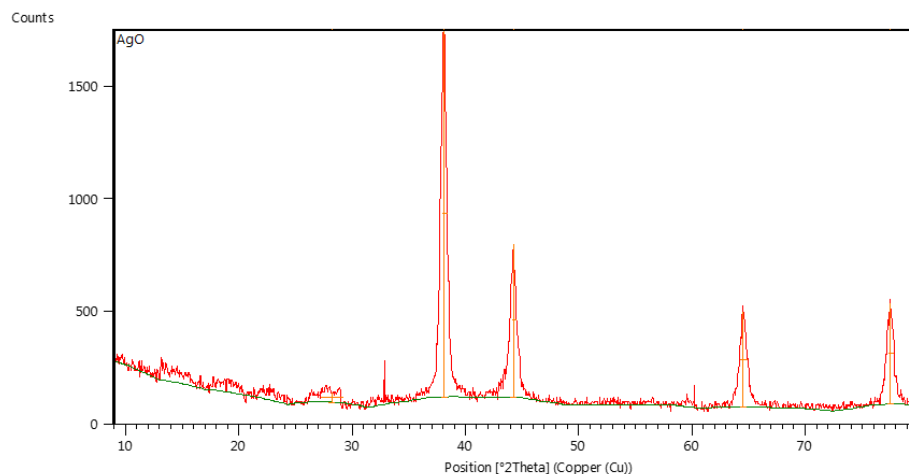


**Figure (8) shows the X-ray diffraction (XRD) spectrum of the prepared silver nanoparticles.**

**Table (2) shows the data of the three strongest XRD bands.**

NO	2Th	I/I1	FWHM	Nanoparticles(nm)
1	38.0676	100	0.492	16.198
2	44.2617	41.03	0.3444	23.14
3	77.537	26.9	0.492	16.198

## Adsorption

### Determination of $\lambda_{max}$ and construction of calibration curves for each safranin dye.

The maximum wavelength of safranin dye, at which the highest absorption occurs, was determined using a UV-Vis spectrometer over a wavelength range of 200-800 nm, using a 1 cm thick quartz cell. The maximum wavelength of safranin dye was determined to be 518 nm. Diluted solutions were prepared at successive concentrations (1, 1.5, 2, 2.5, 3, 3.5, 4, 4.5)  $\times 10^{-5}$  M to estimate the amount of adsorbed and residual safranin dye in the solution using spectrophotometry. A calibration curve was constructed using the aforementioned concentrations. The relationship between absorbance and concentration for safranin dye is shown in Figure (9). The results showed a linear relationship indicating the impression that the system follows according to the Lambert-Burt law.

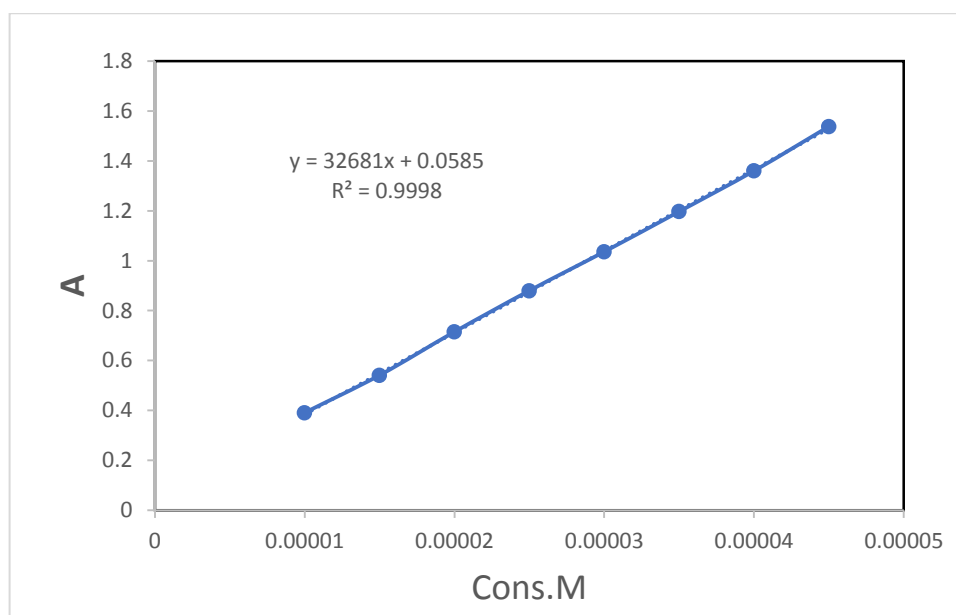


**Figure (9) Calibration curve for safranin dye.**

### Determining the equilibrium time.

To determine the time required for the adsorption system to reach equilibrium, the change in the adsorbent concentration was monitored over time until chemical equilibrium was achieved. The study was conducted using fixed safranin concentrations of  $2.5 \times 10^{-5}$  M and a fixed weight of the adsorbent surface (cellulose) of 0.1 g at 20 °C and a safranin wavelength of 518 nm, as shown in the following table, which illustrates the results obtained.

Adsorption%	Adsorption Capacity $\times 10^{-5}$ (mg/g)	Adsorbed $\times 10^{-5}$ M	Residual $\times 10^{-5}$ M	Absorbance	tim (min)
				0.880	0
65.4	1.635	1.635	0.864	0.341	5
78.7	1.969	1.969	0.530	0.232	10
89.2	2.232	2.232	0.267	0.146	15
92.1	2.302	2.302	0.197	0.123	20
92.1	2.302	2.302	0.197	0.123	25
84.2	2.106	2.106	0.393	0.187	30
77.5	1.938	1.938	0.561	0.242	35

When comparing the absorbance values of the dye before and after the adsorption process using cellulose, it was noted that there is a rapid decrease in the absorbance values at the beginning of adsorption due to the high efficiency of the adsorbent surface (cellulose) as a result of the presence of a large number of active sites on the adsorbent surface. Then the adsorption process begins to gradually decrease over time because the increase in the concentration of the adsorbent material (dyes) leads to the saturation of the active sites on the surface of the adsorbent material (cellulose) that are not occupied by the adsorbent material. This is consistent with the kinetic theory of adsorption [17]. As shown in Figure (10), and through the results that were reached, it became clear that the adsorption process reaches a state of equilibrium within a time period ranging between (20-25 min), which gave the highest adsorption efficiency. At this time, the speed of the adsorption process is equal to the speed of the adsorption process. After that, a slight increase in absorbance and a decrease in the adsorption efficiency are observed. The reason is the repulsion of the dye molecules and their return to the solution as a result of the saturation of the pores. On the cellulose surface, this is in great agreement with previous studies in the field of adsorption [18].

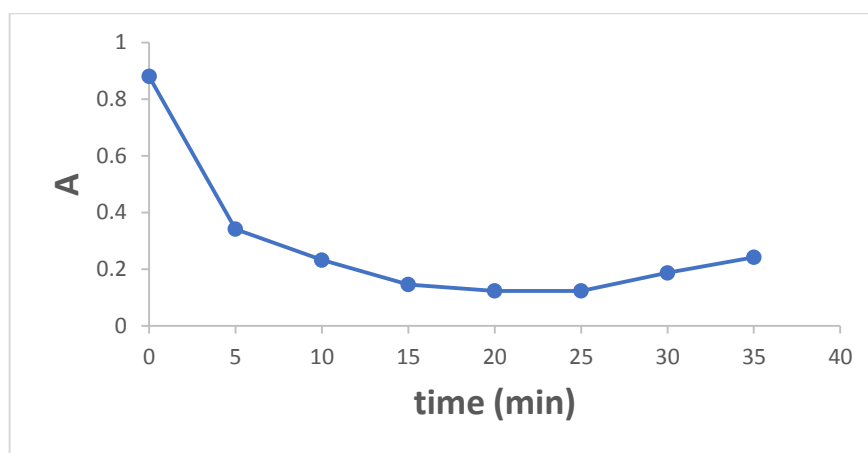


Figure (10) Change in absorption values with time for safranin dye.

### Calculating the thermodynamic functions of adsorption:

Studying the effect of temperature is considered an important study for calculating thermodynamic functions. This is to determine the nature of the adsorption system, the direction in which it proceeds, and the nature of the forces controlling it at equilibrium. The values of the equilibrium constants ( $K_{eq}$ ), used in calculating the thermodynamic functions, were also calculated using the ratio between the adsorbed concentration of safranin dye and the remaining concentration in the solution, as shown in Table (3). A relationship was drawn between the values of  $\ln K_{eq}$  and the reciprocal of temperature ( $1/T$ ), as shown in Figure (11), where the heat of adsorption ( $\Delta H_o$ ) was calculated from the slope of the linear equation according to the van't Hoff equation.

Table (3): The effect of temperature on the equilibrium constant of the adsorption system for safranin dye.

LnKeq	1/T (K <sup>-1</sup> )	Keq	Adsorbed $\times 10^{-5}M$	Residual $\times 10^{-5}M$	A	T (K)
2.456	0.003413	11.667	2.302	0.197	0.123	293
1.793	0.003356	6.013	2.143	0.356	0.175	298
0.776	0.0033	2.172	1.712	0.787	0.316	303
-0.226	0.003195	0.797	1.109	1.390	0.513	313

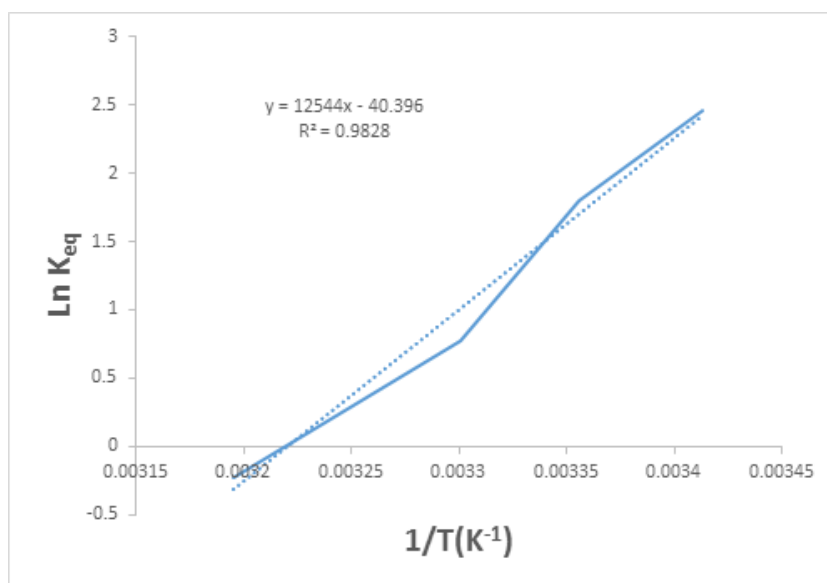


Figure (11) shows the adsorption of safranin dye onto the cellulose surface using the van't Hoff equation.

We note that the value of ( $\Delta H^\circ$ ) is negative, which means that the dye adsorption onto the cellulose surface is an exothermic process and indicates that the adsorption is chemical, as it is higher than 80 KJ/mol. We also note that the adsorption process occurs spontaneously, as the calculated value of ( $\Delta G^\circ$ ) has a negative charge. We can mathematically obtain the value of the change in entropy ( $\Delta S^\circ$ ) using the Gibbs equation, where we note that its value is negative. This is attributed to the fact that the adsorbed and interlocking molecules are less organized (increased randomness) when the adsorption and desorption processes occur together in the solution, as the molecules remain in a state of constant motion. This is consistent with some previous studies [19]. The thermodynamic functions were studied at the optimal adsorption conditions, as shown in Table (4).

**Table (4): Thermodynamic function values for the adsorption of safranin dye onto the cellulose surface at different temperatures.**

T (K)	$\Delta G^\circ$ (J/mol)	$\Delta S^\circ$ (J/mol)	$\Delta H$ (J/mol)
293	-5984.69	-335.51	-104291
298	-4444.61	-335.05	
303	-1955.03	-337.74	
313	588.38	-335.07	

#### Nanosilver loading on cellulose.

##### Determination of Equilibrium Time

The fixed concentration of safranin dye was determined at ( $2.5 \times 10^{-5}$  M), and the optimal weight of the adsorption surface (cellulose) was (0.1 g) at a temperature of (293 K) and a vibration speed of (100 rpm). The wavelength specified for safranin dye was (518 nm). The results showed that the adsorption efficiency of safranin dye in the presence of silver nanoparticles at a concentration of ( $2.8 \times 10^{-5}$  M) reached (85.5%) at an equilibrium time of (20) minutes. When comparing this result with the adsorption efficiency on a cellulose surface without loading, it was noted that the efficiency decreased from (92.1%), but the time required to reach equilibrium remained constant at (20) minutes, as shown in Table (5). Figure (12) shows the change in the adsorption capacity of safranin dye on the cellulose surface over time and in the presence of silver nanoparticles.

**Table (5): Determination of the equilibrium time and adsorption efficiency of safranin dye in the presence of silver nanoparticles (AgNPs) on the cellulose surface.**

%	adsorption capacity ) $q_e$ ( (mg/g)	Adsorbed $\times 10^{-5}$ M	Residual $\times 10^{-5}$ M	A	t (min)
				0.817	0
62.3	1.559	1.559	0.940	0.366	5
70.8	1.770	1.770	0.729	0.297	10
79.1	1.978	1.978	0.521	0.229	15
85.4	2.137	2.137	0.362	0.177	20
85.4	2.137	2.137	0.362	0.177	25
80.7	2.018	2.018	0.481	0.216	30

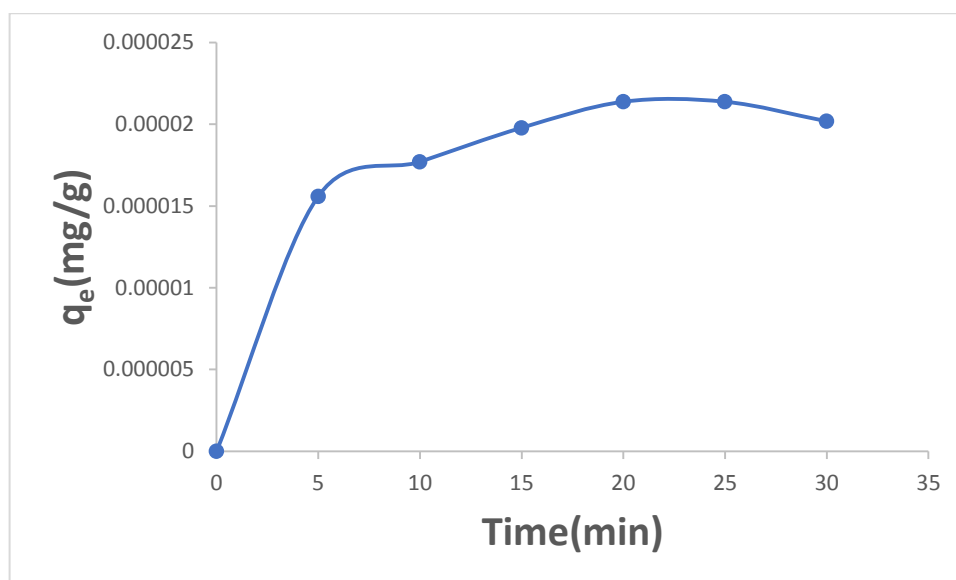


**Figure (12): Change in the adsorption capacity of safranin dye on the cellulose surface over time and in the presence of silver nanoparticles.**

#### Effect of temperature.

The effect of temperature on the adsorption of safranin dye on the cellulose surface was studied in the presence of silver nanoparticles at a concentration of  $(2.8 \times 10^{-5} \text{ M})$  and temperatures of (293, 298, 303, 313), at a constant weight of cellulose (the adsorbent) equal to (0.1 g), a safranin concentration of  $(2.5 \times 10^{-5})$ , and an equilibrium time of (20) minutes, in the presence of silver nanoparticles. The results are documented in Table (6), which shows the change in absorbance at different temperatures. It is noted from Figure (13) that the adsorption efficiency of the safranin dye solution decreases with increasing temperature in the presence of silver nanoparticles. Despite this decrease, the results are still good, achieving a higher adsorption efficiency at 313 K, reaching 67.5% instead of 44.4% for safranin dye.

**Table (6): Effect of temperature on the adsorption efficiency of safranin dye on the cellulose surface in the presence of silver nanoparticles.**

%	adsorption capacity )q <sub>e</sub> ( )mg/g( $\times 10^{-5}$	A	T (K)
85.4	2.137	0.177	293
78.5	1.963	0.234	298
71.2	1.782	0.293	303
67.5	1.687	0.324	313

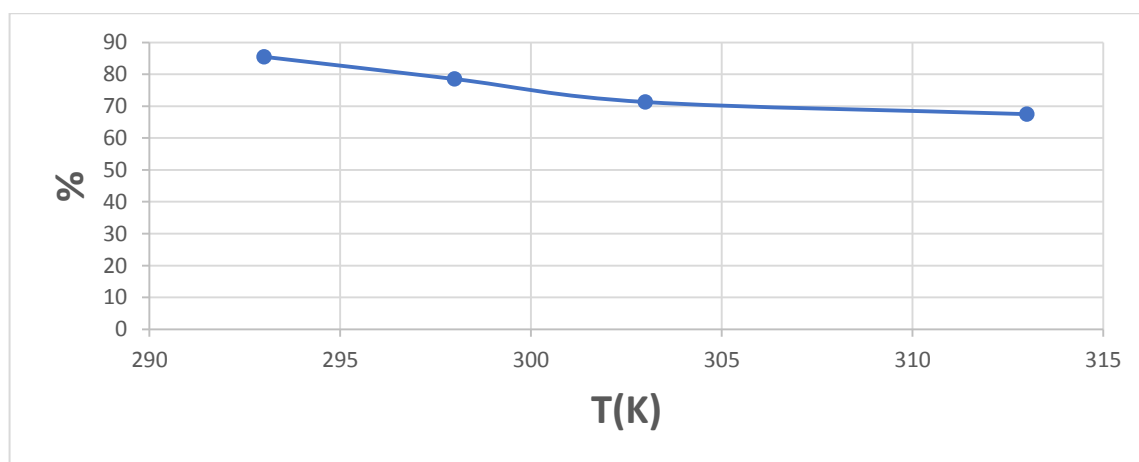


**Figure (13): Decrease in adsorption efficiency with increasing temperature for the adsorption of safranin dye onto the cellulose surface in the presence of silver nanoparticles.**

**Calculating the thermodynamic functions for the adsorption of safranin dye onto the cellulose surface in the presence of silver nanoparticles.**

Table (7) shows the basic thermodynamic functions for the adsorption of safranin dye onto the cellulose surface in the presence of silver nanoparticles. The free energy change ( $\Delta G$ ) and entropy change ( $\Delta S$ ) were calculated. Figure (14) shows the van't Hoff curve for the adsorption of safranin onto the cellulose surface in the presence of silver nanoparticles at a concentration of  $2.8 \times 10^{-5}$  M and at different temperatures. When comparing our results with the previous results before loading, we note that the  $H\Delta$  value decreased from negative (104291 J/mol) to negative (28144 J/mol) for the safranin dye, while the  $\Delta S^0$  values remained negative, and the  $GO\Delta$  values became negative at 313 K after having been positive.

**Table (7): The effect of temperature on the thermodynamic equilibrium constant for the adsorption of safranin dye onto the cellulose surface in the presence of silver nanoparticles ( $2.8 \times 10^{-5}$  M).**

$\Delta S^0$ (J/mol.K)	$\Delta H$ (J/mol)	$\Delta G^0$ (J/mol)	LnKeq	Keq	$1/T$ ( $K^{-1}$ )	T (K)
-81.307	-28144.6	-4321.6	1.774	5.894	0.003413	293
-83.6681	-28144.6	-3211.4	1.296	3.655	0.003356	298
-85.3213	-28144.6	-2292.2	0.909	2.484	0.0033	303
-83.8406	-28144.6	-1902.4	0.731	2.077	0.003195	313

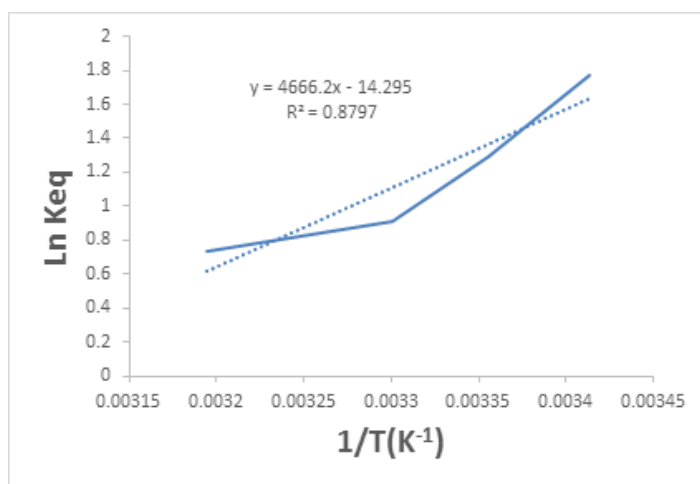


**Figure (14): Van't Hoff curve for safranin adsorption on a cellulose surface in the presence of silver nanoparticles ( $2.8 \times 10^{-5}$  M).**

### Adsorption efficiency.

The previous results show that the adsorption efficiency of safranin dye on a cellulose surface at 293 K before and after loading the silver nanoparticles. However, in this case, we achieved a gain in eliminating bacteria present in contaminated water. We have obtained a hybrid surface capable of adsorbing pollutants and killing bacteria present in water in a new and innovative way through adsorption.

### Conclusions

Silver nanoparticles were successfully synthesized using a natural plant extract, highlighting the importance of plant-based sources as eco-friendly alternatives in nanoparticle fabrication. Various analytical techniques confirmed the formation of uniform silver nanoparticles with an average size of about 18.5 nm, retaining some organic compounds from the extract on the particle surface. The study demonstrated high efficiency in the adsorption of Safranin dye onto cellulose loaded with the nanoparticles, enhancing the potential use of these materials in removing dyes from aqueous solutions. Thermal analyses indicated that the adsorption process is exothermic and spontaneous, accompanied by an increase in internal order during adsorption, suggesting the stability and efficiency of the interaction. The results suggest that using the plant extract to prepare silver nanoparticles not only reduces environmental impact but also improves the adsorption properties, opening new prospects for applications in water treatment.

### References

1. Areej A, Muhammad FM, Somia L, Asifa A, Kainat M, Amna ADMC, et al. 3. Water Pollution and industries. Pure and Applied Biology (PAB), 2020;9(4): 2214-24.
2. Wu H, Gai Z, Guo Y, Li Y, Luz-N Does environmental Pollution inhibit urbanization in China? A new perspective through residents' medical and health costs. Environmental Research. 2020; 182:109128.
3. S. Dubey, S. Banerjee, S.N. Upadhyay, Y.C. Sharma, Application of common nanomaterials for removal of selected metallic species from water and wastewaters: A critical review, J. Mol. Liq. 240(2017) 656-677.
4. K.K. Kefeni, B.B. Mamba, Photocatalytic application of spinel ferrite nanoparticles and nanocomposites in wastewater treatment: Review, Sustain, Mater.Technol. 23 (2020) e00140.
5. K. Nagarajan A. Balaji and N. Ramanujem "Extraction of cellulose nanofibers from *Cocos nucifera* var *aurantiaca* peduncle by ball milling combined with chemical treatment", Carbohydrate Polymers, Vol. 212, PP.312-322, 2019.
6. Agrawal S, Bhatt M, Rai SK, Bhatt A, Dangwal P. Agrawal PK. Silver nanoparticles and its potential applications: A review. J Pharmacogn Phytochem. 2018;7:930-7.
7. Yin IX, Zhang J, Zhao IS, Mei ML, Li Q, Chu CH. The antibacterial mechanism of silver nanoparticles and its application in dentistry. Int J Nanomedicine. 2020; 15:2555.
8. Albanis T.A, Hela D.G., Sakellariades T.M. and Danis T.G., Removal of dyes from aqueous solutions by adsorption on mixtures of fly ash and soil in batch and column techniques, Journal Global Nest Int J, 3(2): 237-244, (2000),
9. Stumm, W, "Chemistry of the solid water interface" John Wiley and Sons, New York, (1992).
10. Ponc , V. Knor, Z., Adsorption of solids, 1<sup>st</sup> , Butterworth, London: (1947)
11. Areej Abed Ar-Rahman Hatteb, "Adsorption of some fluoroquinolones on selected Adsorbents" An-Najeh National, (2010).

12. Saleh J.M., Surface chemistry, 1<sup>st</sup> ed., Bughdad University press, 1-383, (1980)
13. Salvestrini S, Ambrosone L, Kopinke FD. Some mistakes and misinterpretations in the analysis of thermodynamic adsorption data. *J Mol Liq.* 2022;352:118762.
14. Majida HO, Raddia AB, Rajaa AA. Preparation and thermodynamic study of MP2 on the surface of activated charcoal. *Kufa Journal of Chemistry Sciences.* 2013(8).
15. Hulbert BS, Kriven WM. Specimen-displacement correction for powder X-ray diffraction in Debye–Scherrer geometry with a flat area detector. *Journal of applied crystallography.* 2023;56:160-6.
16. Shimojima T, Nakamura A, Ishizaka K. Development of five-dimensional scanning transmission electron microscopy. *Review of Scientific Instruments.* 2023;94(2):023705.
17. Vareda JP. On validity, physical meaning, mechanism insights and regression of adsorption kinetic models. *Journal of Molecular Liquids.* 2023;376:121416.
18. Gnanamoorthy P, Karthikeyan V, Prabu VA. Field Emission Scanning Electron Microscopy (FESEM) characterisation of the porous silica nanoparticulate structure of marine diatoms. *J Porous Mater.* 2014;21:225–33.
19. Cao B, Shen W, Liu Y. Adsorption desulphurization of gasoline by silver loaded onto modified activated carbons. *Adsorpt Sci Technol.* 2008;26(4):225–31.